RSC Advances

PAPER

View Article Online
View Journal | View Issue

Cite this: *RSC Adv.*, 2020, **10**, 17479

Cost-effective smart microfluidic device with immobilized silver nanoparticles and embedded UV-light sources for synergistic water disinfection effects†

Amit Prabhakar, *[a] Mehul Agrawal,[a] Neha Mishra,[c] Nimisha Roy,[a] Ankur Jaiswar,[a] Amar Dhwaj[a] and Deepti Verma*[b]

Received 3rd Januaryu 2020
Accepted 9th April 2020

DOI: 10.1039/d0ra00076k

rsc.li/rsc-advances

A novel microfluidic-device for water disinfection *via* diverse physiochemical effects has been demonstrated. Firstly, a microfluidic device with embedded, multiple germicidal UV-LEDs was fabricated through the innovatively modified cost-effective soft-lithography process. Further, synthesised silver nanoparticles were immobilized within its inner microchannel surface. Disinfection results proved the synergistic bactericidal effect of coated AgNPs and coupled UV-light, while a suspension of bacterial strains, were passed through the micro-device.

The expansion of micro-devices, with different functionalities, is the need of the hour. In particular, cost-effective disinfection of water can profoundly affect the health of the developing world particularly children and is expected to have a huge market. Currently, a large number of water purification systems are commercially available, with effective performance; however, they are exceedingly costly and have heavy maintenance costs for their successful operation. In various distinct approaches a UV light source or silver metal has been used for water purification in large scale water purification systems.

In one of the earlier studies, the antimicrobial activity of a doped hydroxyapatite/polydimethylsiloxane (Ag: HAp-PDMS) composite layer, obtained by the thermal evaporation technique, proved to be active against *Candida albicans*.[1] According to Shekhar Agnihotri *et. al.*, the bacteriostatic/bactericidal effect of AgNPs were size and dose-dependent and for AgNPs.[2] However, in these studies, they did not immobilize the nanoparticles on any surface, rather they have directly used the nanoparticles in suspension-form to conduct the analysis.[2] Ping Y. Furlan *et. al.* designed a bifunctional activated carbon nanocomposite with incorporated nanoscale-sized magnetic magnetite and antimicrobial silver nanoparticles (MACAg) and tested its antimicrobial efficacy against *Escherichia coli* (*E. coli*). They concluded that only Ag nanoparticles and Ag^+ ions showed antimicrobial activities.[3] Joong Hyun Kim *et. al.*, conducted *in situ* fabrication of AgNPs on the surface of PDMS and found the effective antibacterial activity of the nanocomposites against both *E. coli* and *S. aureus*. Also, the nanocomposites were observed to have no cellular toxicity and thus could be used as implants for medical devices.[4] G. Ipek Yucelen and team presented a novel approach to synthesize silver nanoparticles on aluminosilicate nanotubes by decomposition of $AgNO_3$ solution to AgNPs at room temperature and found this hybrid to show strong antibacterial activity towards *Staphylococcus epidermidis* and *Escherichia coli*.[5] The AgNP sheets (AgNPs deposited on the cellulose fibres of an absorbent blotting paper) exhibited antibacterial properties toward suspensions of *Escherichia coli* and *Enterococcus faecalis*, when these pathogenic bacteria were inactivated during percolation through the sheet.[6] A water filter was coated with silver paint to form silver ions (Ag^+) for killing the bacteria present in dirty water and make it drinkable. An overview of nanomaterials for water and wastewater treatment had been recently presented by Haijiao Lu *et al.*[7] Alexandru Rus *et. al.* designed a filter using additive manufacturing techniques and coated it with different concentrations of silver solutions.[8]

The performance of the world's first commercial UV-C LED water disinfection reactor (the Pearl Aqua by Aquisense) was compared with an existing chlorination system and all the tests showed the reactor equivalent to the chlorination system in all aspects.[9] Andrej Gross and team investigated light guidance capabilities of optical pure quartz glass with UV-C LEDs and found the system to show increased disinfection efficiency when tested against *Escherichia coli* and *Bacillus subtilis*.[10] In this approach, they have used the phenomenon of total internal reflection of UV-C irradiation for disinfecting water, in which

[a]*Department of Applied Sciences, Indian Institute of Information Technology Allahabad, Prayagraj, U.P., India. E-mail: amit@iiita.ac.in*

[b]*Department of Chemistry, University of Allahabad, Prayagraj, U.P., India. E-mail: deeptivermachem@gmail.com*

[c]*Department of Electronics & Communication Engineering, Indian Institute of Information Technology Allahabad, Prayagraj, U.P., India*

† Electronic supplementary information (ESI) available. See DOI: 10.1039/d0ra00076k

they have coupled UV-C LEDs to a quartz tube and a glass tube for conducting the analysis.[10]

Further, none of the abovementioned approaches, in earlier reported study, has demonstrated the cumulative disinfection effect of UV-light source, as well as, silver nano-particle, at micro-scale. Unfortunately, none of the existing water disinfection methods provides a crucial combination of key requirements such as high antimicrobial efficiency, low cost, easy maintenance and scalability to both small and large scale. In our premiere approach, a novel cost-effective microfluidic device for water disinfection, with multiple physiochemical effects has been projected in the current study for effective and faster disinfection.

The water disinfection system described here, resolves such problems by providing a simple, cost-effective and efficient water disinfection method with the utilization of silver nanoparticles and ultraviolet (UV) light in a microfluidic system *via* a synergistic effect. The bacteria-infested water was disinfected in the microscopic volumes per unit time. Further, similar multiple microchannels can be arranged in a parallel manner to obtain the required flow rate and quantity of water, needed to be disinfected. The system also ensures safety against silver leakage and excessive human exposure to ultraviolet (UV) light.

Fabrication method

The proposed microfluidic device is fabricated by a customized soft-lithography technique, using PDMS polymer. The height and width of the presented microchannel for the microfluidic device were taken as 500 μm and 300 μm, respectively. Further, as the UV-LEDs were embedded as a side-wall of the same microchannel (with 300 μm width & 500 μm height), hence the dimensions of the UV-LED chambers were identical to the microchannel geometry.

This process requires the fabrication of a SU-8 master mould, using general photolithography process,[11–13] which served as a patterned template for casting PDMS, for creating the desired microstructure. As usual, the initial steps consists of a selection of wafer, SU-8 Spin coating, Pre-Exposure Bake, SU-8 UV-Exposure, Post Exposure Bake, SU-8 Development and Rinse Drying. After the fabrication of the SU-8 master structure, the microchannels of desire dimension in PDMS needs to be formed using a novel procedure. Further, in an original fabrication process, after the fabrication of SU-8 master, a few UV LEDs were securely placed over SU-8 patterned microstructure.

For this purpose, the top/front face of UV-C LEDs were coated with the mixture of 10 : 1 ratio of PDMS pre-polymer & its curing agent, and further semi-cured to make it sticky/gluey. Afterwards, the top-face of UV-C LEDs were glued to the SU-8 master at appropriate places as mentioned in Fig. 1c and d and 5. Subsequently, the mixture of 10 : 1 ratio of PDMS pre-polymer & its curing agent was poured on aforesaid UV-C LEDs glued SU-8 master arrangement; and the whole set-up was cured completely at room temperature for 24 hours (Fig. 1e) to create the final device. Ultimately, the aforementioned prepared PDMS based microdevice was peeled off from the SU-8 master.

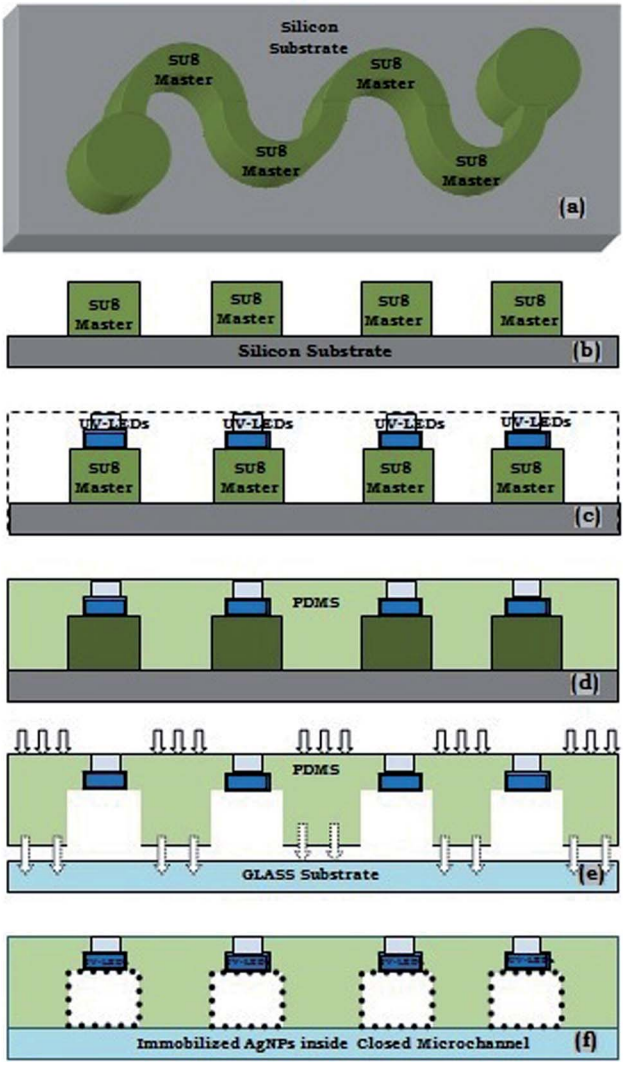

Fig. 1 Schematic diagram for fabrication of device: (a and b) fabricated SU-8 master (c) placement of UV LEDs over SU-8 patterned channel, (d) casting of mixture of 10 : 1 ratio of PDMS pre-polymer and curing agent and further curing this mixture at room temperature for 24 hours. (e) Peeling off the PDMS device from the SU-8 master and, further, bonding on to the glass substrate using semi-cure PDMS layer as adhesive layer. (f) Hydrophilic surface treatment of internal microchannel layer, silanisation, and further AgNPs immobilization on it.

Using this novel approach, a few UV-LEDs were efficiently embedded at various sections of the microchannel (Fig. 1e and 5), for proper coupling of UV rays inside the microchannel, so that appropriate UV disinfection can be made. Furthermore, the fabricated polymer microchannel was sealed with a glass substrate, after making inlet and outlet holes, to create a close microfluidic device (Fig. 1f). The schematic diagram for aforesaid novel fabrication steps of device fabrication is presented in Fig. 1a–f. The fabricated device's microchannels were having 10 cm length and 300 microns channel width.

Reproducibility of the proposed method for micro-device fabrication had been assured by a precisely following photolithography method to create the accurate SU-8 master (for

a potential definite microchannel *via* the soft-lithography process); as well as, scheming a suitable marker in the UV-mask design of SU-8 master, to place the aforesaid LEDs at a definite place in the proposed microchannel during the aforesaid soft-lithography process.

Synthesis of silver nanoparticles

For the synthesis of silver nanoparticles, excessive reducing agent *i.e.* sodium borohydride, $NaBH_4$ is added to silver nitrate, $AgNO_3$ to react in following way:

$$2AgNO_3 + 2NaBH_4 \rightarrow 2Ag + H_2 + B_2H_6 + 2NaNO_3$$

It has been explained in details, in section-1 of ESI.†

In this synthesis, the concentration of silver nanoparticles[14] were 26.95 μg ml^{-1}. The particle size as observed in the system were in between 20.83 nm to 42.10 nm. The optical properties of colloidal silver nano-particle solution were determined in a UV-Vis-spectrophotometer with the appearance in the electronic absorption spectrum of a band located at 396 nm, associated with the presence of small spherical silver nanoparticles.[2]

Several batches of AgNPs suspension were recovered during the synthesis of AgNPs, using the standard protocol.[14,15] Sometimes, due to unfavourable synthesis/storage condition, a high polydispersity of the AgNPs sample appeared (possibly due to aggregation) which is evident with the result of UV-VIS spectroscopy (*i.e.* multiple peaks at around 396 nm and 500 nm) and Dynamic light scattering (Fig. S-3 and S-2 of ESI†). However, the graph revealed only one peak at around 396 nm and no other elongated peaks, under the favourable synthesis/storage condition of AgNPs preparation (Fig. 2e). Additionally, as the disinfection process discussed in our present reported study was based on immobilised AgNPs, hence, any possible variation in the disinfection process was not realized experimentally, in any of the aforesaid cases (*i.e.* either with poly-dispersity of the AgNPs, or with uniform-sized AgNPs). In fact, the AgNPs aggregation process seems to enhance the surface density of AgNPs on the microchannel surface, which may enhance the disinfection efficiency.

AgNPs immobilization protocol followed

The PDMS-microchannel surfaces need to be coated with silver nanoparticles to obtain the effective bactericidal effect of silver nanoparticles. The bactericidal action using contact killing by immobilized AgNPs shows better results than colloidal AgNPs.

To achieve the immobilization of AgNPs inside micro-channel, firstly, the micro-channels are made hydrophilic by flowing the Piranha solution through it, followed by KOH solution treatment[16,17] (Fig. 2 and 3).

Further, quite analogous to earlier reported studies,[14] the microchannel was treated with amino-propyl-tri-ethoxy silane (APTES) for its silanization process, followed by the introduction of AgNPs solution (Fig. 2 and 3).

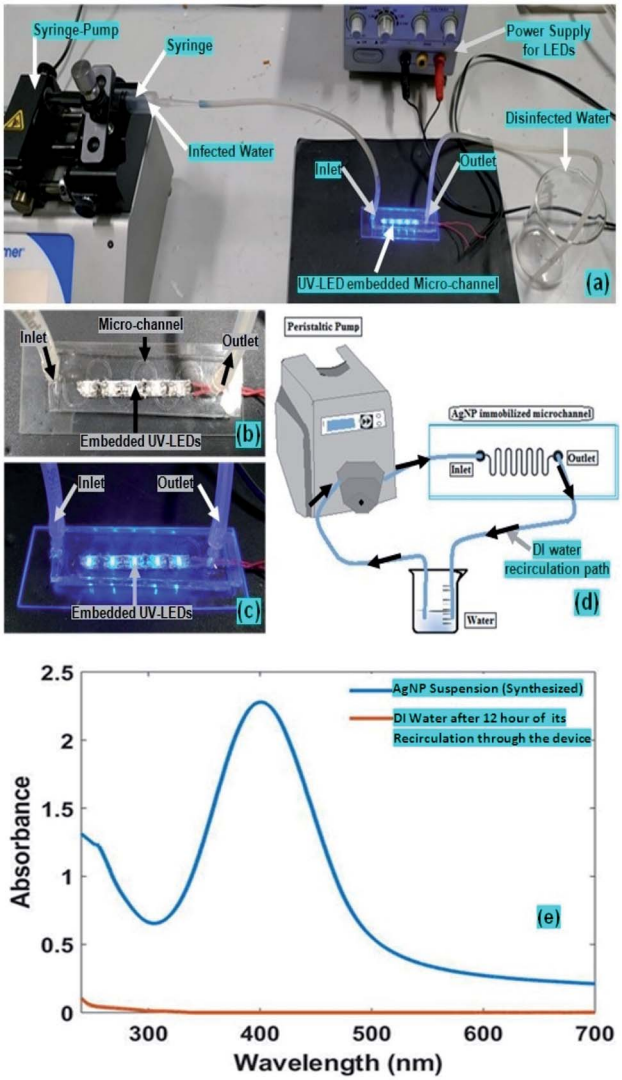

Fig. 2 (a) Experimental Set-up during the treatment of internal wall of device microchannel for creating a hydrophilic surface and AgNPs immobilisation on it; as well as for the general disinfection process; the real picture of: (b) microfluidic device with embedded UV-LEDs; (c) microfluidic device, while LEDs power-supply is switched on; (d) schematic experimental set-up for determining the leaching of the immobilised Ag-NPs from the device's microchannel; (e) UV-Vis spectrum of Synthesized AgNPs and DI Water after 12 hours of its recirculation through the device.

Earlier studies have reported the silanization process performed on PDMS polymer surface also, however, the organo-silane used may be different. In one of the prior study,[15] AgNPs were immobilized on a functionalized glass substrates; *via* the [3-(2-amino-ethyl-amino) propyl] tri-methoxy-silane (AEAPTMS) as a cross-linker molecule (used for silanization process) and then silver nanoparticles were anchored/immobilized on to it.

In another approach, K. Mohammad *et al.*[19] immobilized AgNPs on PDMS surface in a microfluidic chip *via* using 3-amino-propyl-tri-ethoxy silane (APTES), after the oxygen-plasma treatment of PDMS surface. In our present report, PDMS surfaces of microchannel were treated with 2% 3-amino-propyl-tri-ethoxy silane (APTES) solution for its silanization process.

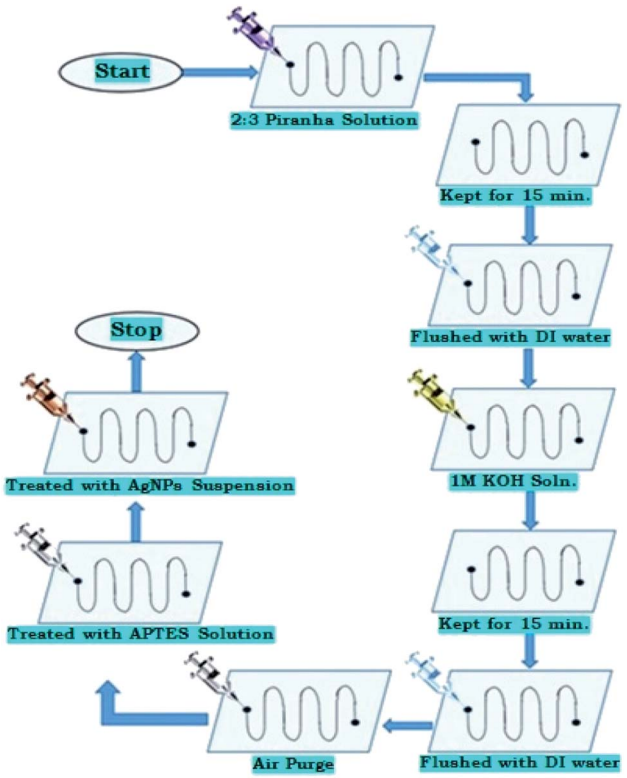

Fig. 3 Flowchart of protocol for hydrophilic surface treatment of PDMS polymer, silanisation, and further AgNPs immobilization on it.

Fig. S-6 (ESI†), presents the schematic of the silanization process for PDMS surface. For aforesaid silanization process, the microchannels were treated with 2% APTES ($C_9H_{23}NO_3Si$) solution for more than 30 minutes, where 2% v/v APTES is prepared in 5 : 2 ethanol to the acetic acid solution,[18,19] which introduces amine functional groups onto the micro-channel surface. Consequently, the silanised PDMS surface of micro-channels was immobilized with AgNPs.

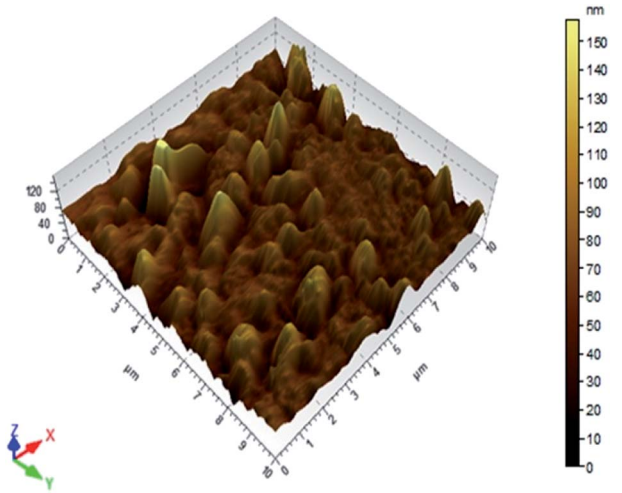

Fig. 4 3D AFM images of AgNPs immobilized PDMS surface of the inner lining of the microfluidic channel.

To confirm the immobilization of AgNPs, the same immobilization protocol was followed on an unsealed replica of PDMS microchannels to get AFM images of untreated PDMS surface and AgNPs-immobilized PDMS surface. The result of 2D & 3D AFM-images is displayed in Fig. 4; as well as, in Fig. S-7.1, S-7.2, S-8.1, S-8.2, S-9.1, S-9.2, S-10.1, and S-10.2 of ESI.† As evidence of proper AgNPs immobilization process, the AgNPs immobilized PDMS surfaces shown higher roughness as compared to plane PDMS surface. However, from the 2D & 3D image (Fig. 4, Fig. S-7.1–10.2 of ESI†), it is apparent that some of the AgNPs immobilised on PDMS surface has more the 100 nm height. In this concern, a very similar metal-nanoparticle immobilisation technique has been elucidated/characterised in our earlier reported studies,[18] which highlight few crucial facts. The theoretical analysis, along with, the experimental validation, in this study,[18] explains the process of aggregation of nanoparticles on the silanised substrate surface, during its immobilisation process. In this reference, it is highly expected that few of the aggregated AgNPs nanoparticles (*i.e.* integer multiple of the average size of an AgNPs *i.e.* up to 40 nm–160 nm…sized aggregates) may appear in AgNPs immobilised surface during its AFM analysis. In fact the AgNPs aggregation process seems to augment the surface density of AgNPs on the PDMS-microchannel surface, which may aid in the disinfection efficiency.

The whole AgNPs immobilisation protocol has been systematically explained, in Section-2 of ESI.†

Moreover, insignificant leaching of the immobilized AgNPs, from the microchannels was observed, while continuously flowing the water (to be disinfected) in microchannel; which is quite similar to earlier reported studies.[15] For determining the leaching of the immobilised Ag-NPs from the device-microchannel, an alternative experimental protocol was adopted; whose schematic set-up, have been elucidated in Fig. 2d. In this process, we pumped a defined 5 ml volume of DI-water (at different flow-rate) through the Ag-NPs coated microchannel, in a cyclic manner (*i.e.* the input & output of -channel were kept at same water reservoir, and DI-water was re-circulated through microchannel *via* the peristaltic micro-pump). Further, after >12 hours of recirculation of DI-water (through the AgNPs coated microchannel), the UV-VIS absorbance-spectra of the re-circulated water sample (collected form aforesaid water reservoir) was recorded. Furthermore, a negligible peak absorbance for the aforesaid absorbance-spectra of flushing/re-circulated DI-water was observed, compared to the prepared Ag-NPs suspension (Fig. 2e). Hence it was realised that an insignificant amount of total silver nanoparticle/ions deposited on the microchannel may leach into the water after 12 hours of extensive flow through the microchannel.

Initial bacterial count and counting living/dead bacteria

Two bacterial strains used for disinfection experiments were Gram-negative, *E. coli* MTCC 443 (ATCC 25922), and Gram-positive, *B. subtilis* MTCC 441 (ATCC 6633). The initial

bacterial count was performed using serial dilution method which showed bacterial colonies for *E. coli* and *B. subtilis* as 7.20 $\times$ 10^7 and 7.28 $\times$ 10^7 CFU ml^{-1} respectively.

This disinfection unit was further tested for the working and the amount of disinfection achieved at the end of the microchannel once the impure water is passed through the unit. The flow rate of impure water was maintained at 0.5 ml min^{-1}, with a target sample output volume of 5 ml to be collected at the outlet in a falcon. For differentiating the living/dead bacteria present in the water sample received at the aforesaid outlet of the micro-device, the PI (Propidium Iodide) "staining method" was used. Propidium iodide is a light-sensitive, fluorescent red nuclear counterstaining dye, which is impermeable to living cells, hence it is used for staining dead cells present in the water-sample to verify the disinfection-efficiency of the microdevice. This dye binds to the DNA of dead cells, and its excitation peak is at 493 nm. The stained samples are then viewed under a fluorescent microscope with a green light source since the absorption maxima of PI (around 496 nm) lies in the wavelength range of green light (495–570 nm) in the visible spectrum. Since PI stains the dead bacterial cells only, they will appear red under the microscope. The procedure for the bacterial count and counting living and dead bacteria, as well as, AgNPs immobilisation protocol has been systematically explained, respectively in Sections 3 and 2 of ESI.†

Water disinfection by UV exposure

To obtain germicidal effect the system were embedded with UV light which in combination with silver nanoparticles provided a synergistic effect when used simultaneously for water disinfection. The UV radiation used for germicidal applications lies in the wavelength range of 100–280 nm. It is called UV-C radiation.[20,21] The peak wavelength for germicidal activity is at 265 nm. Even though the peak wavelength is at 265 nm, but 254 nm is also absorbed by the DNA and RNA.

UV light in this range is absorbed in the DNA and RNA of bacteria. The absorbed UV energy leads to the formation of dimmers by forming new bonds between DNA nucleotides. Dimmer formation, especially thymine, causes major photochemical damage, which stops bacteria from replicating and thus brings disinfection.

The unit of lethal UV-dose is microwatt second per square centimetre ($\mu Ws\ cm^{-2}$) or milli-joule per square centimetre ($mJ\ cm^{-2}$). The lethal UV-dose calculated for the given 7.20 $\times$ 10^7 CFU ml^{-1} and 7.28 $\times$ 10^7 CFU ml^{-1} of *E. coli* and *B. subtilis* suspension, respectively are approximately to be 26.54 $mJ\ cm^{-2}$.

Experimental set-up

The experimental set-up for our disinfection application has been partially presented in Fig. 2. The inlet and outlet of the microfluidic device were coupled respectively with syringe-pump and a collecting-reservoir *via* the silicon tubing. In our presented water disinfection purpose, a microchannel embedded array of 5 UV-C LEDs (30 mW) were used (Fig. 5).

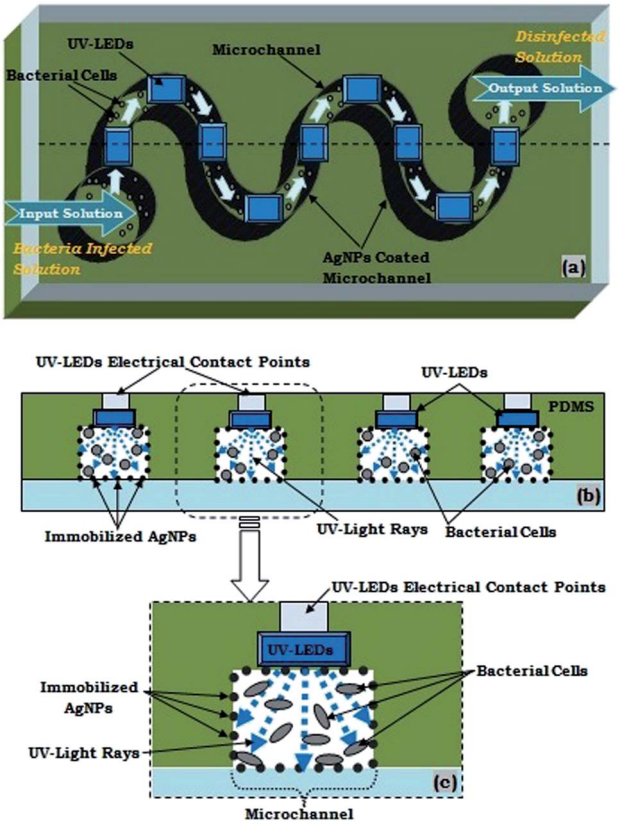

Fig. 5 Schematic diagram AgNPs Immobilized microfluidic device embedded with UV-LEDs, (a) top view: showing the movement of bacterial infected solution from input to output reservoir during the disinfection process; (b) cross-sectional view: showing disinfection process *via* AgNPs contact killing and UV light rays (from UV-LEDs) while the movement of bacterial infected solution from input to output reservoir. (c) Zoomed cross-sectional view: showing bacterial killing process inside a microchannel, *via* AgNPs contact killing and UV light rays.

These set of microchannel coupled UV-LEDs were powered *via* suitable drivers.

A variety of microdevices were fabricated with different numbers of embedded UV-LEDs. However, theoretically as well as experimentally it was realised that only an array of 5 UV-C LEDs (30 mW) were sufficient for the disinfection process. Hence, only 5 UV-C LEDs (30 mW) were switched on (for the devices with more than 5 integrated LEDs); or microdevice with only 5 UV-C LEDs (30 mW) were fabricated.

Moreover, in place of aforesaid microchannel embedded UV LEDs, a different experimental set-up with a single 1 W UV-lamp kept in close vicinity to the fabricated plain AgNPs coated microfluidic chip (made without embedded LEDs), were also utilised. However, disinfection *via* the LEDs embedded microfluidic chip was found more effective, as it required ~8 times lesser optical power than the aforesaid UV-lamp. Which is because in our embedded LEDs based disinfection approach the LEDs were in 10 times closer proximity to the flowing infected water sample.

The flow rate of impure (*i.e.* bacteria-infested) water was maintained at various different rates *i.e.* 0.1 ml min^{-1}, 0.5

ml min^{-1}, 1 ml min^{-1} and 1.5 ml min^{-1}. However, the optimum flow rate for the suitable combined disinfection was found to be at 0.5 ml min^{-1} (Fig. 6). Further, based on the optimum flow rate (*i.e.* 0.5 ml min^{-1}) for disinfection and 0.0045 ml volume of the microchannel, the exposure-time was calculated to be around 0.5 seconds which also agreed with literature.[11] Additionally, at the optimum flow rate (*i.e.* 0.5 ml min^{-1}), the water disinfection *via* only AgNPs coated microchannel and UV-LEDs caused ~94.8% and ~96.7% of bacterial disinfection, respectively. However, the combined effect of AgNPs coated microchannel and UV-LEDs caused ~99.4% disinfection efficiency, at the equivalent optimum flow rate (*i.e.* 0.5 ml min^{-1}).

Results and discussion

It may be assertively understood that both silver nanoparticles and germicidal UV have a synergistic disinfection effect on the bacterial cells, although their disinfection mechanism is entirely different. Silver nanoparticles kill the bacteria by damaging the cell membrane; however, UV-C produces only "point" disinfection which inactivates the bacteria and prevents them from replication. However, when bacterial cells are together treated with both silver nanoparticles and UV-C light then the effect gets multiplied; as the bacteria which remain untreated due to one method could be rendered useless by the other method.

Experimental results indicate that the water disinfection *via* the LEDs embedded microfluidic chip is more effective, as it required ~8 times lesser optical power than the aforesaid UV-lamp. It may be due to the fact that, in our embedded LEDs based disinfection approach, the LEDs were in 10 times closer proximity to the flowing infected water sample. Water disinfection *via* only AgNPs coated microchannel and UV-LEDs caused ~94.8% and ~96.7% of bacterial disinfection, respectively. However, the combined effect of AgNPs coated microchannel and UV-LEDs caused ~99.4% disinfection efficiency, at the same flow rate of bacteria-infested water, through the microdevice. Additionally, the optimum flow rate for AgNPs combined with UV-disinfection were found to be at 0.5 ml min^{-1}.

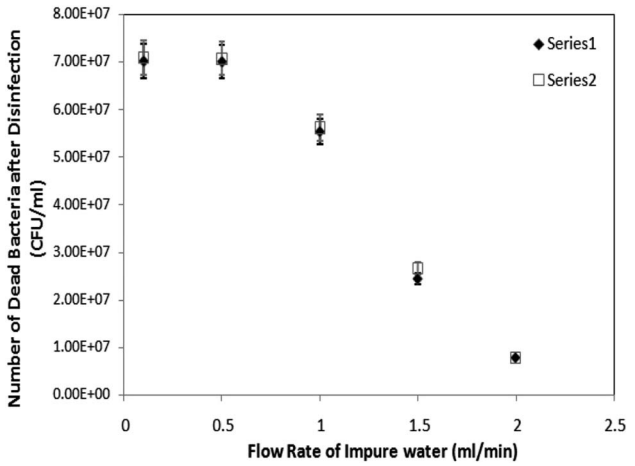

Fig. 6 Showing the disinfection efficiency of the device with UV-disinfection coupled with AgNPs disinfection principle, while the impure water with 7.20×10^7 CFU ml^{-1} (series-1) and 7.28×10^7 CFU ml^{-1} (series-2) of *E. coli* and *B. subtilis*, respectively, were passed through the microfluidic device at different flow rates.

The overall cost of the proposed microdevice is majorly determined by the cumulative cost of related consumables for the complete AgNPs immobilisation process (inside the microchannel); as well as, cost of the items and microfabrication-process for the production of LEDs integrated microdevice. Additionally, as per requirements, the volume-rate for water-disinfection may be scaled-up *via* coupling the multiple units of the proposed device. Simple and economical abovementioned factors, in favour of the reported micro-device (calculated-cost = 5 USD per unit, approx.) reason it to be a 5 to 10 times cost-effective substitute in comparison to any UV-C based water-disinfection unit (present in several existing commercial devices), with comparable sterilization capability [9–10]. Hence, the reported device may be considered as a compact, efficient, as well as, low-cost solution for any similar purpose.

The successful reusability of the micro-device was tested *via* analysing its disinfection efficiency during a cycle of several hours of the disinfection process. It displayed a parallel disinfection capability even after 24 hours of the continuous disinfection process, disinfecting >1000 ml volume (approx.) of infected water. Theoretically, the disinfection capability of the device relied upon the cumulative optical power of the microchannel embedded UV-C LEDs, in addition to, the integrity of immobilized AgNPs on the microchannel surface. Further, the optical power of the embedded UV-C LEDs were observed constant throughout the experiments; as well as, AgNPs leaching experiments (elucidated in Fig. 2d and e) have earlier evidenced about the insignificant leaching of AgNPs (which were immobilised over the microchannel surface), during 12 hours of continuous flow water through the micro-device.

We have observed the maximum disinfection (at the minimum flow-rate *via* the syringe pump *i.e.* 0.5 ml min^{-1}), with the individual effect of AgNPs and UV-LEDs as 95% and 97% respectively; however, with the combination of Ag-NPs and UV-LEDs effects, the percentage disinfection was 99.4% (on average) at same flow-rate. Additionally, we have also observed complete disinfection (*i.e.* up to 99.99%) in most of the experiments with the combination of Ag-NPs and UV-LEDs effects; which seemed improbable with individually either AgNPs or UV-LED based disinfection.

The real gain in the percentage disinfection with the combined effect of Ag-NPs and UV-LEDs, in contrast to, individually either AgNPs or UV-LED may be comprehended as follows. Experimentally, the observed numbers of survived microbes after the abovementioned disinfection process, is almost ~10 times higher for individual AgNPs or UV-LED based disinfection, in comparison to, the disinfection with the combination of Ag-NPs and UV-LEDs effects. The survived microbes after the disinfection process, may have much higher significance if the number density of microbes in the impure input water is 10–100 times higher (*i.e.* 7.2×10^8 to 7.2×10^9 CFU ml^{-1}). Hence, a combination of Ag-NPs and UV-LEDs based disinfection-effects have greatly elevated importance in this aspect.

Conclusion

An innovative water disinfection microdevice has been demonstrated, working *via* diverse physiochemical effects. Initially, a microfluidic device with coupled, multiple germicidal UV-LEDs was fabricated, through the suitably modified cost-effective soft-lithography process. Further, synthesised silver nanoparticles were immobilized inside the microchannel surface *via* an innovative method.

Further, experimentally, both silver nanoparticles and germicidal UV-C were cumulatively found to have a synergistic effect on the bacterial cells present in water, although their disinfection mechanism was entirely different. The microscopic volume of bacteria-infested water was disinfected in its continuous flow. The system also ensures safety against silver leakage and excessive human exposure to ultraviolet (UV) light. In future, multiple microchannels can be arranged in parallel to obtain the required flow rate and quantity of water to be disinfected.

Conflicts of interest

There are no conflicts of interest to be declared.

References

1 C. S. Ciobanu, A. Groza, S. L. Iconaru, C. L. Popa, P. Chapon, M. C. Chifiriuc, R. Hristu, G. A. Stanciu, C. C. Negrila, R. V. Ghita, M. Ganciu and D. Predoi, Antimicrobial Activity Evaluation on Silver Doped Hydroxyapatite/Polydimethylsiloxane Composite Layer, *Bioactive Materials for Bone Tissue Engineering*, 2015, 926513, DOI: 10.1155/2015/926513.

2 S. Agnihotri, M. Soumyo and M. Suparna, Size-controlled silver nanoparticles synthesized over the range 5–100 nm using the same protocol and their antibacterial efficacy, *RSC Adv.*, 2014, **4**, 3974.

3 Y. P. Furlan, A. J. Fisher, A. Y. Furlan, M. E. Melcer, D. W. Shinn and J. B. Warren, Magnetically Recoverable and Reusable Antimicrobial Nanocomposite Based on Activated Carbon, Magnetite Nanoparticles, and Silver Nanoparticles for Water Disinfection, *Inventions*, 2017, **2**(2), 10, DOI: 10.3390/inventions2020010.

4 J. H. Kim, H. Park and S. W. Seo, In situ synthesis of silver nanoparticles on the surface of PDMS with high antibacterial activity and biosafety toward an implantable medical device, *Nano Converg*, 2017, **4**(1), 33, DOI: 10.1186/s40580-017-0126-x.

5 G. Ipek Yucelen, E. Connell Rachel, R. Terbush Jessica, J. Westenberg David and D. Fatih, Synthesis and immobilization of silver nanoparticles on aluminosilicate nanotubes and their antibacterial properties, *Applied Nanoscience*, **6**(4), 607–614, DOI: 10.1007/s13204-015-0467-x.

6 D. Theresa and G. Derek, Bactericidal Paper Impregnated with Silver Nanoparticles for Point-of-Use Water Treatment, *Environ. Sci. Technol.*, 2011, **45**, 1992–1998.

7 H. Lu, J. Wang, M. Stoller, T. Wang, Y. Bao and H. Hao, An overview of nanomaterials for water and wastewater treatment, *Adv. Mater. Sci. Eng.*, 2016, 4964828, DOI: 10.1155/2016/4964828.

8 A. Rus, L. Vasile-Dănu and P. Berce, Silver Nanoparticles (AgNP) impregnated filters in drinking water disinfection, *MATEC Web Conf.*, 2017, **137**, 07007, DOI: 10.1051/matecconf/201713707007.

9 N. M. Hull, W. H. Herold and K. G. Linden, UV LED water disinfection: Validation and small system demonstration study, *AWWA Water Sci.*, 2019, **1**(4), e1148, DOI: 10.1002/aws2.1148.

10 A. Gross, F. Stangl, K. Hoenes, M. Sift and M. Hessling, Improved Drinking Water Disinfection with UVC-LEDs for *Escherichia Coli* and *Bacillus Subtilis* Utilizing Quartz Tubes as Light Guide, *Water*, 2015, **7**(9), 4605–4621, DOI: 10.3390/w7094605.

11 A. Prabhakar and S. Mukherji, Microfabricated polymer analysis chip with integrated U-bend waveguides for evanescent field absorption detection, *Lab Chip*, 2010, **10**, 748–754.

12 A. Prabhakar and S. Mukherji, Investigation of the effect of curvature on sensitivity of bio/chemical sensors based on embedded polymer semicircular waveguides, *Sens. Actuators, B*, 2012, **171–172**, 1303–1311.

13 A. Prabhakar, N. Mishra and S. Mukherji, A Comprehensive Investigation of a Microfabricated U-Bend Polymer Waveguide With Analyte Micro-Reservoir for Versatile On-ChipSensing Applications, *J. Microelectromech. Syst.*, 2017, **26**(4), 935–945.

14 R. U. Mamun, H. K. Md. Bhuiyam and E. M. Quayum, Synthesis of Silver Nano Particles (Ag-NPs) and their uses for Quantitative Analysis of Vitamin C Tablets, *Dhaka Univ. J. Pharm. Sci.*, 2013, **12**(1), 29–33.

15 A. Shekhar, M. Soumyo and M. Suparma, Immobilized silver nanoparticles enhance contact killing and show highest efficacy: elucidation of the mechanism of bactericidal action of silver, *Nanoscale*, 2013, **5**, 7328.

16 D. Maji, *Study of hydrophilicity and stability of chemically modified PDMS surface using piranha and KOH solution*, 19th April, 2011.

17 J. Chin, *et al.*, Quantitative Studies on PDMS-PDMS Interface Bonding with Piranha Solution and its Swelling Effect, *Micromachines*, 2012, **3**, 427–441, DOI: 10.3390/mi3020427.

18 A. Prabhakar and S. Mukherji, A novel C-shaped, gold nanoparticle coated, embedded polymer waveguide for localized surface plasmon resonance based detection, *Lab Chip*, 2010, **10**, 3422–3425.

19 A. Al-Mahmnur, K. Mohammad, D. D. Trung, H. K. Sang, K. H. Young, K. M. Kyung and K. M. Gyu, *Fabrication of Silver Nanoparticles Immobilzed Microfluidic Chip for Chemiluminescence based Analytical Application*, IMCS2012.

20 ClorDiSys, "Ultraviolet Light Disinfection Data Sheet".

21 N. Vermeulen, *The Bactericidal Effect of Ultraviolet and Visible Light on Escherichia coli*, August 6, 2007.